Biochimie 93 (2011) 369–375

Contents lists available at ScienceDirect

Biochimie

journal homepage: www.elsevier.com/locate/biochi

Research paper

Functional and structural evaluation of cysteine residues in the human arsenic (+3 oxidation state) methyltransferase (hAS3MT)

Xiaoli Song [a], Zhirong Geng [a], Xiangli Li [a], Qun Zhao [a], Xin Hu [b], Xinrong Zhang [c], Zhilin Wang [a,*]

[a] State Key Laboratory of Coordination Chemistry, School of Chemistry and Chemical Engineering, Nanjing University, Hankou Road 22, Nanjing 210093, PR China
[b] Modern Analysis Center of Nanjing University, Nanjing 210093, PR China
[c] Key Laboratory for Atomic and Molecular Nanosciences of Education Ministry, Department of Chemistry, Tsinghua University, Beijing 100084, PR China

ARTICLE INFO

Article history:
Received 14 July 2010
Accepted 14 October 2010
Available online 30 October 2010

Keywords:
Cysteine residues
Human arsenic methyltransferase
Structure-function roles
Thermotropic properties

ABSTRACT

Arsenic (+3 oxidation state) methyltransferase (AS3MT) catalyzes the methylation of inorganic arsenic (iAs) and plays important role in the detoxication of this metalloid. There are fourteen cysteine residues in the human AS3MT (hAS3MT), among which twelve are absolutely conserved; Cys334 and Cys360 are unique; Cys368 and Cys369 are identified as a CysCys pair. The roles of several conserved cysteine residues in rat AS3MT and hAS3MT have been reported. Herein, the other conserved cysteine residues (Cys72, Cys271, Cys375) and the unique ones (Cys334, Cys360) were systematically replaced by serine using site-directed mutagenesis to study their functions. The mutants were investigated for enzymatic activity, kinetics, thermal stability and secondary structures. Present results indicate that C72S is completely inactive in methylation of iAs and has distinct changes in the secondary structures; Cys72 might form a critical intramolecular disulfide bond with Cys250; Cys271 and Cys375 do not affect the activity and structure of the hAS3MT. However, the mutations of Cys334 and Cys360 can decrease the enzymatic turnovers and change the conformation of the hAS3MT. The kinetic data show that Cys271, Cys334, Cys360 and Cys375 are not involved in the SAM binding. Additionally, all these cysteine residues except Cys375 affect the thermotropic properties of the hAS3MT.

1. Introduction

The arsenic (+3 oxidation state) methyltransferase (AS3MT) has been known well for its important roles in the metabolism of inorganic arsenic (iAs) in many species [1–4]. Large inter-individual variation in arsenic metabolism was observed [5–7], which may be due to the genetic polymorphisms of the enzymes participating in this process. AS3MT catalyzes the transfer of a methyl group from the donor S-adenosyl-L-methionine (SAM) to arsenic (+3) substrate, producing methylated arsenicals. This process might inactivate biologically active and toxic arsenicals. During the reaction, AS3MT requires a reductant for its catalytic activity, such as glutathione (GSH) [8]. At present, the mechanism of the AS3MT has been summarized into two different reaction schemes. One is described as a metabolic pathway incorporating oxidative methylation and the cycling reduction of pentavalent arsenicals to trivalent states [9–11]. Another has been reported by Hayakawa et al. [12] as successive methylation without oxidation in the presence of glutathione (GSH).

Previous studies implicated cysteine (Cys) residues in enzymatic functions, such as the maintenance of enzyme structure and the regulation of enzyme activity. Yeates et al. reported that Cys residues played critical roles in the structural stabilization of intracellular proteins in thermophiles by forming disulfide bond [13]. In bacteria, Cys residues were found to be involved in the reduction reaction of arsenate to arsenite [14]. Cys157 and Cys207 were proved to be the active sites of the recombinant mouse AS3MT [15]. Our previous data also indicated that the replacement of Cys156, Cys206 and Cys250 with serine completely abolished enzymatic activity of the hAS3MT. Cys156 and Cys206 were the active sites of the hAS3MT. Cys250 might be essential for the maintenance of the hAS3MT stability by forming an intramolecular disulfide bond with another Cys residue. Nevertheless, Cys226 did not affect the activity and structure of the enzyme [16]. In addition,

Abbreviations: iAs, inorganic arsenic; MMA, monomethylated arsenicals; DMA, dimethylated arsenicals; AS3MT, arsenic (+3 oxidation state) methyltransferase; BSA, bovine serum albumin; Isopropyl, β-d-thiogalactopyranoside (IPTG); SAM, S-adenosylmethionine; GSH, glutathione; CD, circular dichroism; ATR-FTIR, attenuated total reflection fourier transform infrared; WT, wild-type; HPLC–ICP–MS, high performance liquid chromatography–inductively coupled plasma-mass spectrometry; SDS-PAGE, sodium dodecyl sulfate-polyacrylamide gel electrophoresis.

* Corresponding author. Tel.: +86 25 83686082; fax: +86 25 83317761.
E-mail address: wangzl@nju.edu.cn (Z. Wang).

0300-9084/$ – see front matter © 2010 Elsevier Masson SAS. All rights reserved.
doi:10.1016/j.biochi.2010.10.010

Thomas et al have reported the roles of some conserved Cys residues (32, 61, 85, and 156) in the N-terminal region of the recombinant rat AS3MT. The mutation of Cys156 completely inactivated the enzyme [1]. In the C-terminal portion of the AS3MT, common to rat, mouse, and human, there are another seven conserved Cys residues, including a CysCys pair. The human enzyme also has unique Cys residues at 334 and 360. However, the roles of these Cys residues have not been studied.

In order to understand the roles of all the Cys residues in the hAS3MT, we used site-directed mutagenesis to substitute the remaining Cys residues with serine to investigate the properties of the mutants. The mutated enzymes were characterized with respect to their activity, kinetics towards arsenite (iAs^{3+}) and SAM. The secondary structures of the mutants were monitored by circular dichroism (CD) and attenuated total reflection fourier transform infrared (ATR-FTIR). Furthermore, the thermostability of the WT hAS3MT and mutated enzymes was also studied. The roles of each Cys residue were systematically documented.

2. Materials and methods

Caution: Inorganic arsenic [17] is recognized as human carcinogen. It should be used accordingly.

2.1. Materials

Unless otherwise noted, all reagents are analytical grade or better. Arsenicals were bought from J&K Chemical Ltd. Restriction enzymes, dNTPs and PrimeSTAR HS DNA Polymerase were from Takara. The wild-type (WT) hAS3MT expression plasmid (pET-32a-hAS3MT) was available from an earlier study [18]. Expression host (*Escherichia coli* BL21 (DE3) pLysS) was got from Novagen. Bovine serum albumin (BSA), S-adenosyl-L-methionine (SAM), isopropyl β-D-thiogalactopyranoside (IPTG), and glutathione (GSH) were all bought from Sigma. All solutions were prepared with Milli-Q deionized water. The phosphate buffered solution (PBS) was prepared from Na_2HPO_4 and NaH_2PO_4.

Stock solutions containing each of the following species (1000 mg As/L) were prepared in Milli-Q deionized water: arsenite and arsenate prepared from $NaAsO_2$ (iAs^{3+}) and $Na_2HAsO_4{\cdot}7H2O$ (iAs^{5+}), respectively; methylarsonate prepared from disodium methylarsonate (MMA); dimethylarsinate prepared from dimethylarsinic acid (DMA) (J&K Chemical Ltd.). All the stock solutions were stored at 4 °C in the dark. Working solutions of standards were prepared fresh daily from the stock solutions.

2.2. Site-directed mutagenesis and protein expression

Site-directed mutagenesis of the hAS3MT was performed directly on the cDNA encoding for the hAS3MT in the plasmid pET-32a-hAS3MT [16,18]. Substitutions of Cys72, Cys271, Cys334, Cys360 and Cys375 of the hAS3MT for serine were carried out using the PCR megaprimer or PCR overlap extension method with pET-32a-hAS3MT as the DNA template. *E. coli* BL21 (DE3) pLysS was used for protein production. The primers used for mutagenesis are listed in Table 1, with the mutated codons bold and underlined. The oligonucleotide primers, each complementary to opposite strands of the hAS3MT gene sequence, were extended during temperature cycling (30 cycles of PCR consisting of incubation for 10 s at 95 °C, 15 s at 56 °C, and 1 min at 72 °C) and final extension (7 min at 72 °C) by using PrimeSTAR HS DNA Polymerase. PCR products were double-digested using *Eco*RV and *Sal*I restriction endonucleases, and cloned into the prepared *Eco*RV/*Sal*I-digested pET-32a-hAS3MT expression vector. DNA sequencing of the hAS3MT mutants was carried out by using the double-stranded dideoxy method to ensure that no errors had been introduced during the amplification process [19]. For expression, the vectors carrying the mutant hAS3MT genes were transformed into *E. coli* BL21 (DE3) pLysS. Single colonies selected on standard ampicillin-containing agar plates were picked. Protein expression and purification followed the protocols described previously [16,18]. Differently, to obtain substantial soluble protein of C72S, lower temperature (20 °C), lower concentration of IPTG (0.3 mM) and long induction time (overnight) were needed. The purified proteins were identified by SDS-PAGE. Then the protein solution was dialyzed four times against PBS (25 mM, pH 7.0) at 4 °C. Protein concentration was determined by the method of Bradford [20] based on a BSA standard curve.

Table 1
Primers used for site-directed mutagenesis.

	Primer	Sequence
C72S	−	5′-CCA**GCT**GTTTTCTAGATGCTC-3′
C271S	+	5′-GACAGGACCAACCAAGAGA**AGC**-3′
	−	5′-GTAAATAACTTG**GCT**TCTCTTGG-3′
C334S	+	5′-CATCTGGAGGC**AGC**TCTGCTTTG-3′
C360S	+	5′-CAGTATGAAGTCCAGATG**AGC**CCC-3′
C375S	−	5′-GTCGACTTAGTGATGGTGATGGTGATG**GCT**GC-3′
Universal	+	5′-CGGGATATCATGGCTGCACTTCGTGAC-3′
	−	5′-CGGGTCGACTTAGTGATGGTGATG-3′

Bold letters indicate the mutation sites introduced by PCR-based mutagenesis.
(+) sense strand; (−) antisense strand.

2.3. Steady-state enzyme activity assays and kinetic measurements

The steady−state activity of the WT hAS3MT and the mutants was determined by HPLC-ICP-MS in the standard assay system (100 μl) containing 11 μg enzyme, 7 mM GSH, 1 μM iAs^{3+} and 1 mM SAM in PBS (25 mM, pH 7.0) [16,18,21,22]. For the kinetics, various concentrations of iAs^{3+} (0.5−500 μM) and SAM (0.05−2 mM) were used. The enzyme incubations were carried out at 37 °C for times indicated in the figures. Then the samples were treated with H_2O_2 at a final concentration of 3% to convert all arsenic metabolites to pentavalency [12]. The H_2O_2-treated samples were boiled for 5 min and centrifugated at 12000 rpm for 10 min to remove the denatured protein. After being filtered though a 0.22 μm pore membrane, 20 μl aliquots of samples were analyzed by HPLC-ICP-MS (PRP X-100 250 mm × 4.6 mm i.d., 5 μm, Hamilton/Elan9000) with a flow rate of 1.2 ml/min at room temperature. The pH of the mobile phase (15 mM $(NH_4)_2HPO_4$) was adjusted to 6.0 with H_3PO_4. The amounts of arsenic species were calculated with the working curves prepared using 5, 10, 20, 40, 80 and 160 ppb of standard arsenic species. Methylation rates were calculated as mole equivalents of methyl groups transferred from SAM to iAs^{3+} (i.e., 1 pmol CH_3 per 1 pmol MMA or 2 pmol CH_3 per 1 pmol DMA) [23]. The rate of methylation fit to the noncompetitive substrate inhibition [24] Eq. (1):

$$V = [S]^{*}V\max/\left(K_M + [S] + [S]^2/K_I\right). \quad (1)$$

Here, V is the initial velocity of the reaction (pmolCH_3transferred/h/mg protein); [S], the substrate (iAs^{3+}) concentration (μM); Vmax, the maximal velocity of the reaction (pmolCH_3transferred/h/mg protein); K_M, the Michaelis constant for iAs^{3+} (μM); K_I, the inhibition constant for iAs^{3+} (μM) [25].

2.4. Circular dichroism measurements and secondary structure analysis

CD (190−260 nm) spectra were recorded on a JASCO-J810 Spectropolarimeter (Jasco Co., Japan) in a cell with 1 mm light length at room temperature. The scanning rate was set at 50 nm/

min and the spectra were the average of four readings of a very dilute enzyme solutions (4 μM). Baseline correction was automatically carried out with the PBS (25 mM, pH 7.0) spectrum during the complete collection time. The secondary structure parameters of the mutants were computed by using Jwsse32 software with reference of CD-Yang. Jwr [26].

2.5. ATR-FTIR spectroscopy and secondary structure analysis

ATR-FTIR spectra were measured with an infrared spectrometer (Bruker, IFS 66/s) equipped with a deuterated triglyceride sulphate (DTGS) detector and an ATR device at room temperature. The employed protein concentration was 1.0×10^{-4} M in PBS (25 mM, pH 7.0). An open background spectrum was recorded previously and then the protein solution was spread on the ZnSe wafer. Spectrum was collected at a resolution of 4 cm^{-1}. The water vapor and CO_2 correction was automatically carried out during data collection. Protein spectrum was obtained by subtracting the spectrum of PBS (25 mM, pH 7.0). Baseline correction and curve-fitting processes were performed in amide Iband (1600–1700 cm^{-1}) by origin software (version 7.0) to get the best Gaussian-shaped curves that fit the original protein spectrum. Secondary derivative was applied to estimate the position and strength of the component bands. Assignment and integration of each component band gave the relative contents of different types of secondary structures.

2.6. Thermotropic properties of the activity and structure of hAS3MT

The thermotropic properties of the WT hAS3MT and the Cys/Ser mutants were characterized at 45 °C. The assay mixtures (400 μl) containing 44 μg enzyme, 1 μM iAs^{3+}, 1 mM SAM, 7 mM GSH in PBS (25 mM, pH 7.0) were incubated at 45 °C. Aliquots (100 μl) were removed at various times and were treated with H_2O_2 before analyzed by HPLC-ICP-MS. All measured activities were normalized as percentage of control activity (37 °C). In addition, the secondary structures of the hAS3MT and the mutants were monitored by CD spectroscopy at different temperatures (0, 25, 37 and 45 °C). Before measurement, the protein solutions were incubated for 20 min at each temperature. For 37 °C and 45 °C, the secondary structures of the enzymes were also detected at different times corresponding to the activity assays.

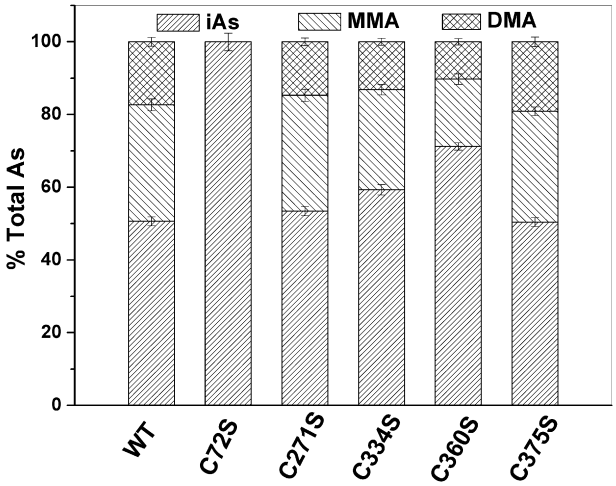

Fig. 1. Catalytic activity of the hAS3MT mutants. Reaction mixtures (100 μl) containing 11 μg enzyme, 1 μM iAs^{3+}, 1 mM SAM, 7 mM GSH in PBS (25 mM, pH 7.0) were cultured at 37 °C for 1.5 h with H_2O_2 treatment before analyzed by HPLC–ICP–MS. Values are the means ± S.D. of three independent experiments.

3. Results and discussion

3.1. Catalytic activity and kinetics of the hAS3MT mutants

In an effort to assess whether the mutation of individual Cys residue affects the overall methylation capacity of hAS3MT, we carried out a comprehensive investigation of the activity and kinetic properties of the mutants. The amounts of each arsenical were calculated from the working curves with the Chromera software as described previously[16,18]. Among these mutants, C72S completely abolished enzymatic activity. The activity of C334S and C360S decreased. However, no significant changes were observed in the activity of C271S and C375S (Fig. 1). These results indicate that Cys72 plays important roles in enzyme function. Cys334 and Cys360 are also important for hAS3MT. In contrast, Cys271 and Cys375 are not concerned with catalysis directly.

The kinetics of the active hAS3MT mutants was investigated towards a wide iAs^{3+} and SAM concentration range. Substrate inhibition of rate by iAs^{3+} was observed for all the active mutants in the concentration range studied (Fig. 2A). The kinetic constants of the active mutants estimated by fitting the Eq. (1) are shown in

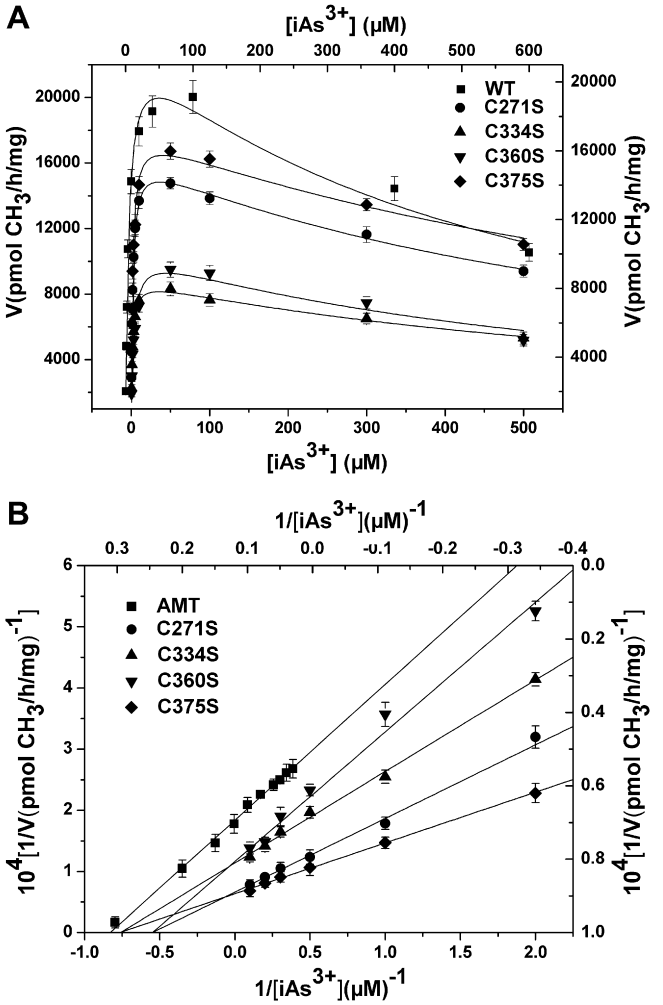

Fig. 2. (A) Dependence of the enzymatic activity of WT [16] and mutant hAS3MT on the concentration of iAs^{3+}. The lines show the least squares fit of Eq. (1) to the data. (B) Double reciprocal plots of the relation between the concentration of iAs^{3+} and the rate. Reaction mixtures (100 μl) containing 11 μg enzyme, 1 mM SAM, 7 mM GSH in PBS (25 mM, pH 7.0) were incubated with the concentrations of iAs^{3+} indicated for 1.5 h with H_2O_2 treatment before analyzed. The data for the WT hAS3MT are on the top and right axes. Values are the means ± S.D. of three independent experiments.

Table 2
Kinetic parameters for iAs^{3+} methylation by the WT hAS3MT [16] and mutants.

	K_M (μM)[a]	K_I (mM)[a]	Vmax (pmol/h/mg)[a]	K_M (μM)[b]	Vmax (pmol/h/mg)[b]	K_M (μM)[c]
WT	3.20	0.70	21170	3.19	19836	47.8
C271S	1.88	0.70	16376	1.98	15743	51.2
C334S	1.60	0.78	8877	1.31	8849	50.3
C360S	2.32	0.67	10657	2.02	9336	49.5
C375S	1.85	0.82	17979	1.59	16691	49.0

[a] Represents the kinetic parameters of iAs^{3+} estimated from the data in Fig. 2A by Eq. (1) using origin 8.0.
[b] Represents the kinetic parameters of iAs^{3+} calculated from the data in Fig. 2B.
[c] Represents the K_M of SAM.

Table 2. Double reciprocal plots were also employed to calculate the kinetic parameters (Fig. 2B). As shown in Table 2, these two methods give the consistent results. The K_I values for all the active mutants are similar to that for the WT hAS3MT while the values of K_M decrease. The *V*max values of C271S and C375S are similar to that of the WT hAS3MT. However, the *V*max values of C334S and C360S decrease (WT hAS3MT: K_M, 3.2 μM; K_I, 0.7 mM; *V*max, 19836 pmol/h/mg [16]). These kinetic data further illuminate that Cys271 and Cys375 do not influence the activity of the hAS3MT while Cys334 and Cys360 might play potential roles in the enzyme function.

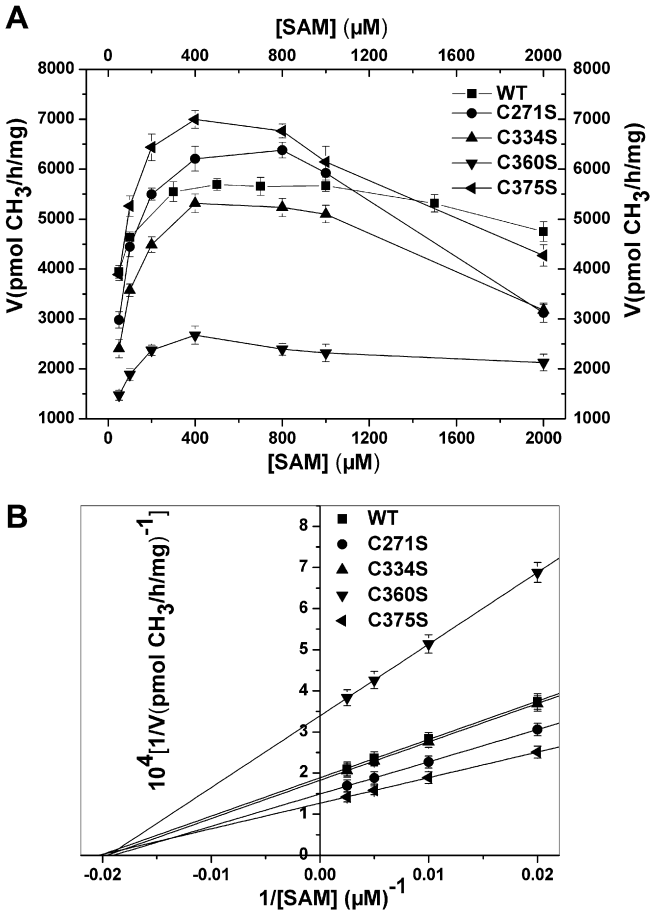

Fig. 3. (A) Dependence of the enzymatic activity of WT [16] and mutant hAS3MT on the concentration of SAM. The data for the WT hAS3MT are on the top and right axes. (B) Double reciprocal plots of the relation between the concentration of SAM and the rate. Reaction mixtures (100 μl) containing 11 μg enzyme, 1 μM iAs^{3+}, 7 mM GSH in PBS (25 mM, pH 7.0) were incubated with the concentrations of SAM indicated for 1.5 h with H_2O_2 treatment before analyzed. Values are the means ± S.D. of three independent experiments.

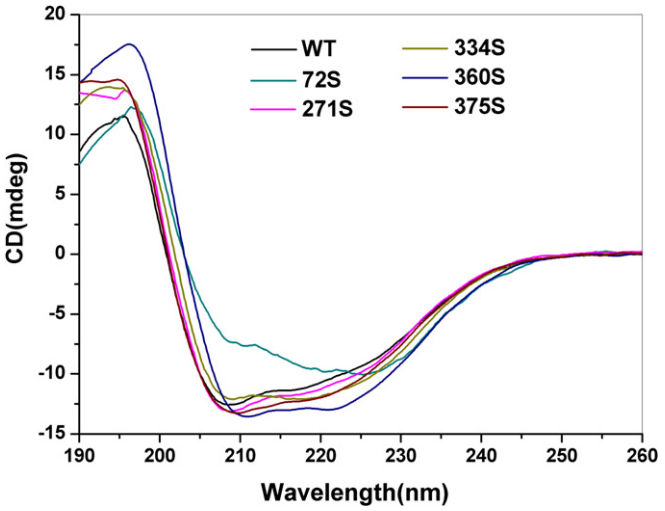

Fig. 4. CD spectra of the WT hAS3MT and the mutants. Spectra were taken at protein concentration of 4 μM at room temperature. Plot is the representative of four independent measurements.

The relationship between the SAM concentration ([SAM]) and the methylation rate is shown in Fig. 3A. With [SAM] increasing, the methylation rate increased. However, inhibition was also observed for all the active mutants at higher SAM concentrations. The K_M values of SAM calculated from the double reciprocal plots (Fig. 3B) are also shown in Table 2. For all the active mutants, the K_M values of SAM are similar to that of the WT hAS3MT (WT: 47.8 μM [16]). These data reveal that Cys271, Cys334, Cys360 and Cys375 are not involved in the SAM binding.

3.2. Secondary structures of the mutants determined by circular dichroism and ATR-FTIR

Cys residues are usually conserved and play important role in the structure and function of proteins [27,28]. The mutation of Cys250 absolutely ruined the structure of the hAS3MT, resulting in the loss of the enzymatic activity. Thus, Cys250 was speculated to form a disulfide bond with another Cys residue [16]. To find the potential Cys residue bonding with Cys250 and to see the structural roles of the Cys residues, we monitored the conformation of the mutants by CD and ATR-FTIR spectroscopy. As shown in Fig. 4, the CD spectra of C271S and C375S are similar, and resemble that of the WT hAS3MT. C334S exhibits a similar spectrum with C360S but is different from

Table 3
Secondary structures of the WT [16] and mutant hAS3MT estimated from CD spectra (A), FTIR spectra (B).

	α%	β%	Turn%	Random%
A				
WT	29.0 ± 2.2	23.9 ± 1.9	17.9 ± 1.7	29.2 ± 1.4
C72S	45.3 ± 2.3	0	28.9 ± 1.5	25.8 ± 1.9
C271S	28.9 ± 1.3	27.6 ± 2.0	17.3 ± 1.1	26.2 ± 2.6
C334S	33.9 ± 1.9	19.8 ± 0.9	19.1 ± 1.7	27.2 ± 1.8
C360S	34.0 ± 2.4	18.8 ± 1.3	20.4 ± 1.9	26.7 ± 2.3
C375S	28.5 ± 1.1	24.6 ± 2.6	17.6 ± 1.5	29.3 ± 1.4
B				
WT	26.6 ± 3.6	20.7 ± 4.6	24.2 ± 3.2	28.5 ± 4.9
C72S	41.3 ± 2.3	4.40 ± 0.4	30.4 ± 3.3	23.9 ± 1.7
C271S	29.9 ± 0.7	24.0 ± 2.4	21.2 ± 1.8	24.9 ± 1.6
C334S	33.0 ± 3.4	19.5 ± 1.2	21.5 ± 2.6	26.0 ± 0.9
C360S	32.5 ± 1.3	21.0 ± 1.7	24.8 ± 2.7	21.7 ± 0.8
C375S	28.1 ± 1.4	25.2 ± 1.9	21.9 ± 2.0	24.8 ± 1.5

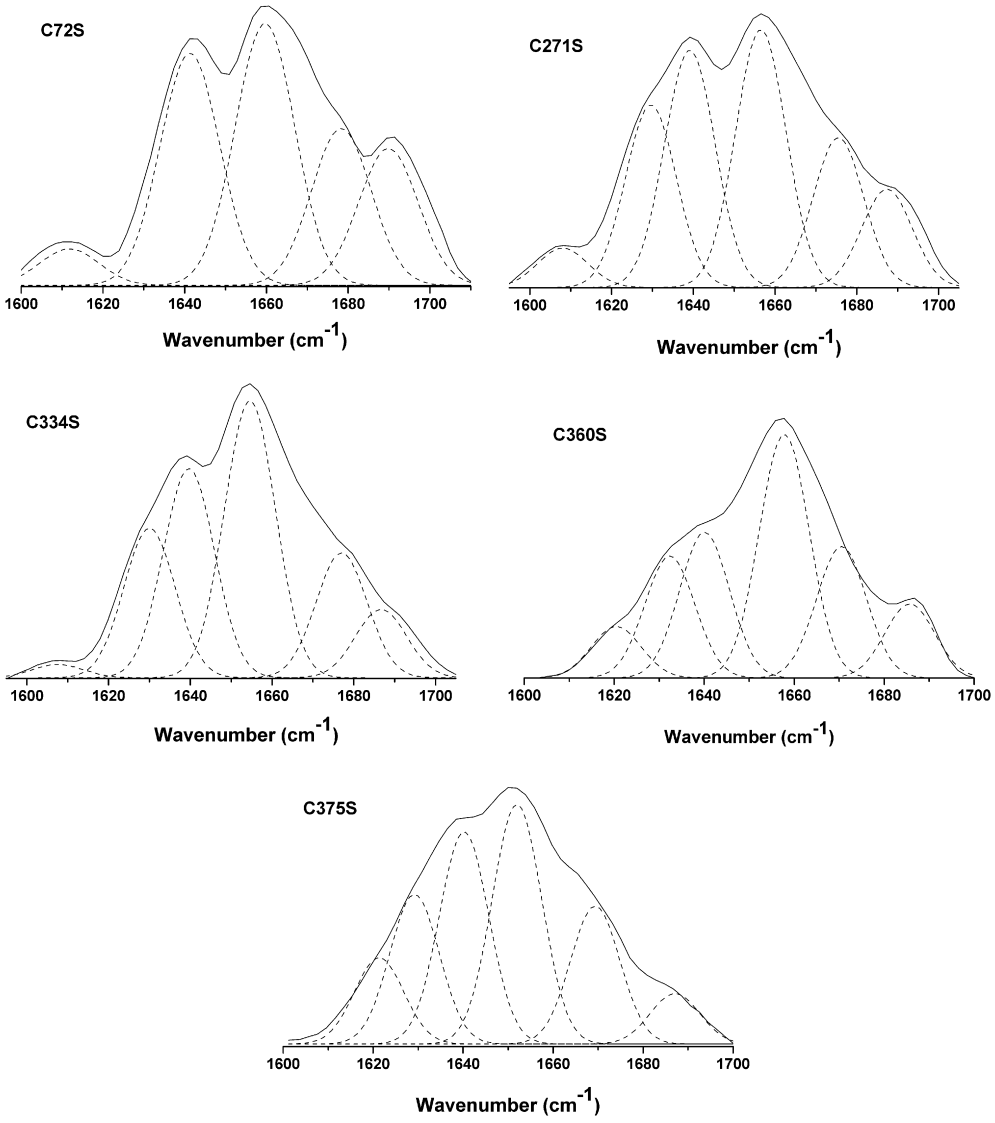

Fig. 5. Curve-fitted amide I region of the mutants. The component peaks are the result of curve-fitting using a Gaussian shape. The solid lines represent the experimental FTIR spectra after Savitzky–Golay smoothing; the dashed lines represent the fitted components. Plot is the representative of three independent measurements.

the WT hAS3MT. For the CD spectra of C334S and C360S, the intensity of the 208 nm peak decreases while the intensity of the 220 nm peak increases as compared with that of the WT hAS3MT. However, distinctly different changes are detected in the spectrum of C72S, the peak at 208 nm almost disappears and the intensity of the whole spectrum dramatically decreases. The secondary structures from the CD spectra were computed by Jwsse32 software with reference of CD-Yang. Jwr (Table 3A) [26]. The WT hAS3MT was estimated to have 29.0% α-helix, 23.9% β-pleated sheet, 17.9% β-turn, and 29.2% random coil [18]. The secondary structures of C271S and C375S are almost the same with that of the WT hAS3MT. The contents of α-helix in C334S and C360S have a respective increase of 16.9% and 17.2%, while the contents of β-pleated sheet decrease by 17.2% and 21.3%, respectively. Surprisingly, there is no β-pleated sheet reserved in the C72S, and the contents of α-helix and β-turn increase by 56.2% and 61.0%, respectively.

The amide I band (about 1600–1700 cm^{-1}) in the FTIR spectrum mainly attributes to the C=O stretching vibrations of the amide groups, and is sensitive to the secondary structures of proteins, enzymes and polypeptides [29–31]. In order to further confirm the structures of the mutants, we analyzed the amide I band of their FTIR spectra. Fig. 5 shows the original and curve-fitting FTIR spectra of the mutants. There are six component bands in the amide I band of the mutants except C72S. Obviously, the FTIR spectra of C271S and C334S are similar with that of C375S and C360S, respectively. Nevertheless, the spectrum of C72S is very different and only has five component bands. According to the well-established assignment criterion (1610–1640 cm^{-1} to β-pleated sheet, 1640–1650 cm^{-1} to random coil, 1650–1658 cm^{-1} to α-helix, and 1660–1700 cm^{-1} to β-turn) [32], the contents of each secondary structure of the mutants were obtained from the integrated areas of the component bands (Table 3B). For C72S, the band at 1659 cm^{-1} was empirically assigned to the α-helix [33], and this is similar to C250S [16]. It can be seen that the secondary structures of the mutants estimated from the FTIR and CD spectra are in close agreement with each other.

We have reported that there was only 2.3% β-pleated sheet in C250S and α-helix increased to 43.7%. Summarizing these results, we can see that the shape of the CD spectra and the secondary structures of C250S and C72S are similar to each other. In addition, both mutants are inactive in the methylation of iAs^{3+}, and both need lower temperature, lower concentration of IPTG, but long

induction time to get substantial soluble forms. Then we can surmise that Cys250 may form an intramolecular disulfide bond with Cys72, and this bond plays a very important role in supporting the hAS3MT structure. Cys334 and Cys360 might form hydrogen bonds with other residues and/or solvent water, or disulfide bond with each other. However, these bonds might not be essential to the structure maintenance. In contrast, Cys271 and Cys375 do not affect the hAS3MT structure.

3.3. Thermotropic properties of WT hAS3MT and the mutants

Site-directed mutagenesis is usually used to separate the local interaction of individual residue that plays important roles in the global structure of proteins. Mutational replacement of residues often leads to temperature-sensitive mutants, and the study of the thermotropic properties of these mutants generally provides considerable information [34,35]. Thus, we designed an assay to examine the thermotropic properties of the mutants to further determine the roles of the Cys residues in hAS3MT. C271S and C226S were less thermally stable than the native form during all the incubation time (Fig. 6). C334S was more thermally stable than the WT hAS3MT within 30 min incubation and then rapidly lost its activity. Particularly, C360S was a little more stable than the native form. However, the activity of C375S was similar with that of the WT hAS3MT during heat treatment.

Considering the relationship between the structure and activity of enzymes, we also analyzed the structure of these active mutants at 0, 25, 37 and 45 °C, respectively. With temperature increasing, α-helix almost had no changes in C271S and C226S, while β-pleated sheet decreased. For C375S, both α-helix and β-pleated sheet had a little increase while β-turn and random coil decreased. This pattern is similar with that of the WT hAS3MT. The α-helix in C360S first decreased and then increased as temperature increased, contrarily, the β-pleated sheet first increased and then decreased. However, the α-helix in C334S decreased and β-pleated sheet increased with temperature increasing. The changes in structures correspond with the changes in activities of the mutants. The secondary structures of the WT hAS3MT and the mutants almost did not change at 37 °C with various incubation times. However, for the incubation at 45 °C, the α-helix had a little increase while the β-pleated sheet decreased for the WT and all the mutants. These results further indicate that Cys375 does not affect the thermotropic properties of the hAS3MT. Nevertheless, the mutation of the other Cys residues might alter the interactions of amino acids surrounding, resulting in the difference in the thermotropic properties of the mutants. The data may also indicate that the enzymatic activity is directly related to the β-pleated sheet in the hAS3MT. These findings are similar to our results from the spectroscopy and the kinetics.

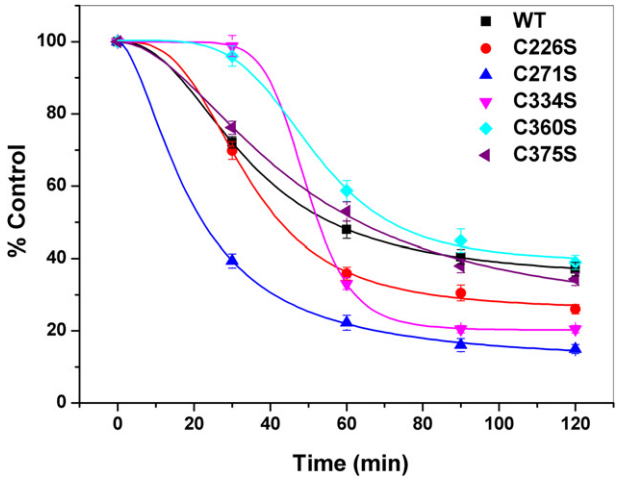

Fig. 6. Thermotropic properties of the WT hAS3MT and the mutants. Reaction mixtures (400 μl) containing 44 μg enzyme, 1 μM iAs^{3+}, 1 mM SAM, 7 mM GSH in PBS (25 mM, pH 7.0) were incubated at 45 °C while control samples were kept at 37 °C. Aliquots were removed at various times for analysis to determine the enzyme activity. All measured activities were normalized as a percentage of control activity. Values are the means ± S.D. of three independent experiments.

4. Conclusions

In summary, our systematic study has revealed the roles of the Cys residues in hAS3MT. Cys72 might form an intramolecular disulfide bond with Cys250, which is essential in maintaining the hAS3MT structure; Cys271 and Cys375 do not affect the activity and structure of the enzyme; Cys334 and Cys360 have some effects on the function of the hAS3MT, the mutation of these two residues decreased the enzymatic turnovers. Based on all of the previous works, we can conclude that Cys72, Cys250, Cys156 and Cys206 are critical functional residues in the hAS3MT; Cys32, Cys61, Cys85, Cys226, Cys375 and Cys271 are not concerned with the enzyme functions; to some extent, Cys334 and Cys360 can affect the activity and structure of the hAS3MT.

Acknowledgements

This work is supported by the National Natural Science Foundation of China (21075064, 21027013, 20721002 and 90813020), the National Basic Research Program of China (2007CB925102) and the Key Research Program of ministry of Education of China (105081).

References

[1] J.X. Li, S.B. Waters, Z. Drobna, V. Devesa, M. Styblo, D.J. Thomas, Arsenic (+3 oxidation state) methyltransferase and the inorganic arsenic methylation phenotype, Toxicol. Appl. Pharmacol. 204 (2005) 164–169.
[2] E. Wildfang, T.R. Radabaugh, H.V. Aposhian, Enzymatic methylation of arsenic compounds. IX. Liver arsenite methyltransferase and arsenate reductase activities in primates, Toxicology 168 (2001) 213–221.
[3] R.A. Zakharyan, H.V. Aposhian, Enzymatic reduction of arsenic compounds in mammalian systems: the rate-limiting enzyme of rabbit liver arsenic biotransformation is MMA^V reductase, Chem. Res. Toxicol. 12 (1999) 1278–1283.
[4] E. Wildfang, R.A. Zakharyan, H.V. Aposhian, Enzymatic methylation of arsenic compounds, Toxicol. Appl. Pharmacol. 152 (1998) 366–375.
[5] M. Vahter, Genetic polymorphism in the biotransformation of inorganic arsenic and its role in toxicity, Toxicol. Lett. Vols.112–113 (2000) 209–217.
[6] K.S. Engström, K. Broberg, G. Concha, B. Nermell, M. Warholm, M. Vahter, Genetic polymorphisms influencing arsenic metabolism: evidence from Argentina, Environ. Health. Perspect. 115 (2007) 599–605.
[7] J.S. Chung, D.A. Kalman, L.E. Moore, M.J. Kosnett, A.P. Arroyo, M. Beeris, D.N. Mazumder, A.L. Hernandez, A.H. Smith, Family correlations of arsenic methylation patterns in children and parents exposed to high concentrations of arsenic in drinking water, Environ. Health Perspect. 110 (2002) 729–733.
[8] R. Zakharyan, Y. Wu, G.M. Bogdan, H.V. Aposhian, Enzymatic methylation of arsenic compounds: assay, partial purification, and properties of arsenite methyltransferase and monomethylarsonic acid methyltransferase of rabbit liver, Chem. Res. Toxicol. 8 (1995) 1029–1038.
[9] W.R. Cullen, B.C. McBride, J. Reglinski, The reaction of methylarsenicals with thiols: some biological implications, J. Inorg. Biochem. 21 (1984) 179–194.
[10] W.R. Cullen, B.C. McBride, J. Reglinski, The reduction of trimethylarsine oxide to trimethylarsine by thiols: a mechanistic model for the biological reduction of arsenicals, J. Inorg. Biochem. 21 (1984) 45–60.
[11] H.V. Aposhian, Enzymatic methylation of arsenic species and other new approaches to arsenic toxicity, Annu. Rev. Pharmacol. Toxicol. 37 (1997) 397–419.
[12] T. Hayakawa, Y. Kobayashi, X. Cui, S. Hirano, A new metabolic pathway of arsenite: arsenic-glutathione complexes are substrates for human arsenic methyltransferase Cyt19, Arch. Toxicol. 79 (2005) 183–191.
[13] M. Beeby, B.D. O'Connor, C. Ryttersgaard, D.R. Boutz, L.J. Perry, T.O. Yeates, The genomics of disulfide bonding and protein stabilization in thermophiles, PLoS Biol. 3 (2005) 1549–1558.

[14] R. Mukhopadhyay, B.P. Rosen, Arsenate reductases in prokaryotes and eukaryotes, Environ. Health Perspect. 110 (2002) 745–748.
[15] D.E. Fomenko, W.B. Xing, B.M. Adair, D.J. Thomas, V.N. Gladyshev, High-throughput identification of catalytic redox-active cysteine residues, Science 315 (2007) 387–389.
[16] X.L. Song, Z.R. Geng, J.S. Zhu, C.Y. Li, X. Hu, N.S. Bian, X.R. Zhang, Z.L. Wang, Structure-function roles of four cysteine residues in the human arsenic (+3 oxidation state) methyltransferase (hAS3MT) by site-directed mutagenesis, Chem. Biol. Interact. 179 (2009) 321–328.
[17] T. Kuroki, T. Matsushima, Performance of short-term tests for detection of human carcinogens, Mutagenesis 2 (1987) 33–37.
[18] Z.R. Geng, X.L. Song, Z. Xing, J.L. Geng, S.C. Zhang, X.R. Zhang, Z.L. Wang, Effects of selenium on the structure and function of recombinant human S-adenosyl-L-methionine dependent arsenic (III) methyltransferase in *E. coli*, J. Biol. Inorg. Chem. 14 (2009) 485–496.
[19] F. Sanger, S. Nicklen, A.R. Coulson, DNA sequencing with chain-terminating inhibitors, Proc. Natl. Acad. Sci. U S A 7 (1977) 5463–5467.
[20] M.M. Bradford, A rapid and sensitive method for the quantitation of microgram quantities of protein utilizing the principle of protein-dye binding, Anal. Biochem. 72 (1976) 248–254.
[21] J. Gailer, S. Madden, W.R. Cullen, M.B. Denton, The separation of dimethylarsinic acid, methylarsonous acid, methylarsonic acid, arsenate and dimethylarsinous acid on the Hamilton PRP-X100 anion-exchange column, Appl. Organometal. Chem. 13 (1999) 837–843.
[22] G. Raber, K.A. Francesconi, K.J. Irgolic, W. Goessler, Determination of 'arsenosugars' in algae with anion-exchange chromatography and an inductively coupled plasma mass spectrometer as element-specific detector, Fresenius. J. Anal. Chem. 367 (2000) 181–188.
[23] F.S. Walton, S.B. Waters, S.L. Jolley, E.L. LeCluyse, D.J. Thomas, M. Styblo, Selenium compounds modulate the activity of recombinant rat As^{III}-methyltransferase and the methylation of arsenite by rat and human hepatocytes, Chem. Res. Toxicol. 16 (2003) 261–265.
[24] G.L. Kedderis, A.R. Elmore, E.A. Crecelius, J.W. Yager, T.L. Goldsworthy, Kinetics of arsenic methylation by freshly isolated B6C3F1 mouse hepatocytes, Chem. Biol. Interact. 16 (2006) 139–145.
[25] W.W. Cleland, Steady state kinetics. in: P.D. Boyer (Ed.), The Enzymes, vol 2. Academic Press, New York, 1970, pp. 1–65.
[26] Y.T. Yang, C.S.C. Wu, H.M. Martinez, Calculation of protein conformation form circular dichroism, Meth. Enzymol. 130 (1986) 208–257.
[27] T. Kamata, H. Ambo, W. Puzon-Mclaughlin, K.K. Tieu, M. Handa, Y. Ikeda, Y. Takada, Critical cysteine residues for regulation of integrin αIIbβ3 are clustered in the epidermal growth factor domains of the β3 subunit, Biochem. J. 378 (2004) 1079–1082.
[28] J.C. Reese, B.S. Katzenellenbogen, Mutagenesis of cysteines in the hormone binding domain of the human estrogen receptor, J. Biol. Chem. 266 (1991) 10880–10887.
[29] A. Dong, P. Huang, W.S. Caughey, Redox-dependent changes in β-extended chain and turn structures of cytochrome *c* in water solution determined by second derivative amide I infrared spectra, Biochemistry 31 (1992) 182–189.
[30] W.K. Surewicz, H.H. Mantsch, New insight into protein secondary structure from resolution-enhanced infrared spectra, Biochim. Biophys. Acta 952 (1988) 115–130.
[31] S. Krimm, J. Bandekar, Vibrational spectroscopy and conformation of peptides, polypeptides, and proteins, Adv. Protein Chem. 38 (1986) 181–364.
[32] D.M. Byler, J.N. Brouillette, H. Susi, Quantitative studies of protein structure by FTIR spectral deconvolution and curve fitting, Spectroscopy 3 (1986) 29–32.
[33] A.C. Dong, W.S. Caughey, Infrared methods for study of hemoglobin reactions and structures, Methods Enzymol. 232 (1994) 139–175.
[34] D.T. Suzuki, Temperature-sensitive mutations in *drosophila melanogaster*, Science 170 (1970) 695–706.
[35] J.C. Reese, B.S. Katzenellenbogen, Characterization of a temperature-sensitive mutation in the hormone binding domain of the human estrogen receptor. Studies in cell extracts and intact cells and their implications for hormone-dependent transcriptional activation, J. Biol. Chem. 267 (1992) 9868–9873.